

# CEINCI-LAB. A free software to find the seismic capacity curve of frames with ADAS or TADAS dissipators

## CEINCI-LAB un software libre para hallar la curva de capacidad sísmica de pórticos con disipadores ADAS o TADAS

R. Aguiar <sup>1\*</sup>, D. Mora <sup>\*\*</sup>, M. Rodríguez <sup>\*</sup>

\* Universidad de Fuerzas Armadas ESPE, Quito. ECUADOR

\*\* Escuela Politécnica Nacional, Quito. ECUADOR

Fecha de Recepción: 21/08/2015

Fecha de Aceptación: 28/11/2015

PAG 37-53

### Abstract

CEINCI-LAB is a computer software developed using MATLAB for static or dynamic structural analysis, in a friendly way and simultaneously serves the user to reinforce structural knowledge. In this article the most important aspects are present to find the resistant seismic capacity curve of a reinforced concrete or steel plane frame, with ADAS or TADAS energy dissipators above Chevron Braces, using the Pushover technique. To whole dissipating-brace system two models are shown, the first is by two equivalent braces and the second is considering the dissipating element like a short element. For this last case, the dissipating element is analyzed in two ways, to the first the dissipating element stiffness matrix is found and to the second some rectangular segments of constant section are considered to model the dissipating element.

*Keywords:* ADAS or TADAS energy dissipator, chevron braces, pushover

### Resumen

CEINCI-LAB es un sistema de computación desarrollado en MATLAB que permite realizar el análisis estático o dinámico de estructuras, en forma amigable y a la vez sirve para que el usuario pueda afianzar sus conocimientos estructurales. En este artículo se presentan los aspectos más importantes para hallar la curva de capacidad sísmica resistente de un pórtico plano de hormigón armado o de acero, con disipadores de energía ADAS o TADAS que se hallan sobre contravientos Chevron, empleando la Técnica del Pushover. Para el conjunto contraviento-disipador se presentan dos modelos de análisis, el uno es mediante dos diagonales equivalentes y en el otro al elemento disipador se lo considera como un elemento corto. Para éste último caso, el elemento disipador es analizado de dos maneras, en la primera se encuentra la matriz de rigidez del elemento disipador y en la segunda se consideran varias dovelas rectangulares de sección constante para el elemento disipador.

*Palabras clave:* Disipadores de energía ADAS o TADAS, contraviento chevrón, técnica del pushover

## 1. Introduction

One way to systematically reinforce structures is with the use of ADAS (Added damping and stiffness) or TADAS (Triangular plate added damping and stiffness) dissipating devices on steel Chevron braces, as shown in Figure 1 (Whittaker et al. 1989; Tsai et al. 1993). The ADAS are made up of steel plates in the shape of an hour-glass, with dimensions  $b_1$  in the widest part and  $b_2$  in the narrowest section; whereas the shape of the TADAS is triangular with dimension  $b$ , in the widest part; in the case of the two dissipating devices,  $h$  is the height of the dissipating device and  $t$  is the thickness of one of the plates that may be steel or alloys of copper, zinc and aluminum (Heresi, 2012).

The shape of the ADAS dissipating devices allows the entire element to have plastic flexural double curvature and TADAS has a simple curvature. (Aguiar et al., 2015; Chistopoulous C. y Filiatraul A., 2006). These dissipating devices increase the structural damping and rigidity

This article presents the most important aspects of the use of the CEINCI-LAB computer system to obtain the resistant seismic capacity curve of concrete or steel frame, placing the dissipating devices mentioned on Chevron braces (in the shape of an inverted V); applying the monotonic pushover technique was use, applying lateral pressure to each floor until the structure reaches the point of collapse.

<sup>1</sup> Corresponding Author:

Profesor Principal. Dr. en Ing., graduado en la Universidad Politécnica de Cataluña. M.Sc, en Ing. sísmica, graduado en la Universidad Central de Venezuela. Ing. Civil, graduado en la Politécnica Nacional. Vicepresidente del Instituto Panamericano de Geografía e Historia IPGH  
E-mail: rraguiar@espe.edu.ec



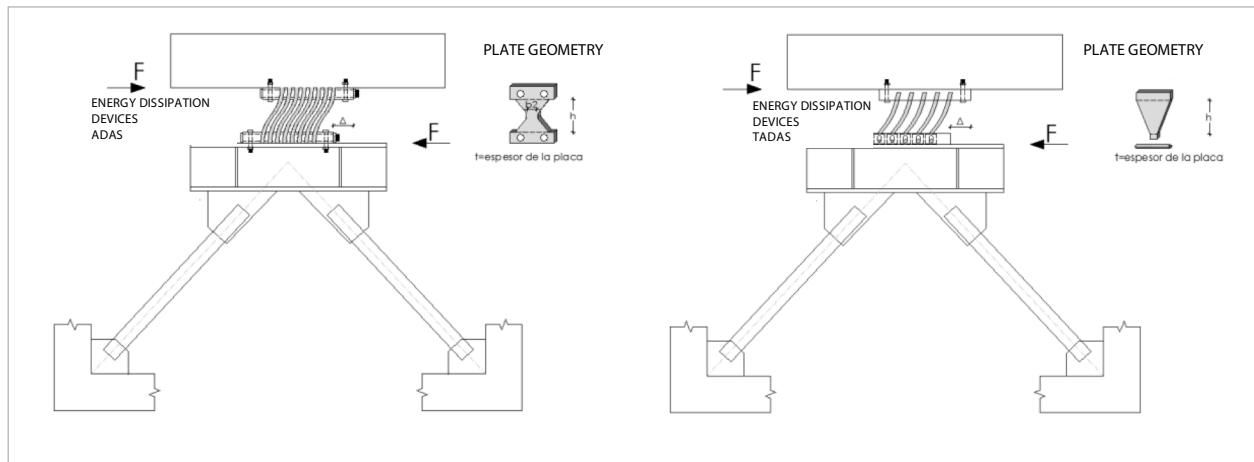


Figure 1. ADAS (right) and TADAS (left) energy dissipating devices on steel Chevron braces

## 2. Models of dissipating devices-braces

The upper part of Figure 2 presents the model of the equivalent brace; it actually involves two braces that are used with the brace-dissipating device set.

$$\frac{1}{K_{eq}} = \frac{1}{K_{DIAG}} + \frac{2 \cos^2 \theta}{K_{EDDE}} \quad (1)$$

Where  $K_{eq}$  is the equivalent axial rigidity of one of the braces;  $K_{DIAG}$  is the axial rigidity of the steel brace;  $K_{EDDE}$  is the secant rigidity (effective) of the bilinear diagram that defines the performance of the dissipating device;  $\theta$  is the angle formed by the equivalent brace on the horizontal axis. (Whitaker et al., 1989).

The lower part of Figure 2 shows that the brace-dissipating device set is composed of three elements: two steel braces and a dissipating device element. To the right of the figure, the global coordinates system is indicated for each of the elements; the steel brace is an element of flat support (Kotulka (2007), y AISC-360, 2010.)

The two forms of the element's rigidity matrix, known as A and B, were found for the dissipating element. In the first form the rigidity matrix was found to be an element in the variable section, whose geometry is defined by the ADAS or TADAS dissipating devices (see Figure 3.) (Tena 1997).

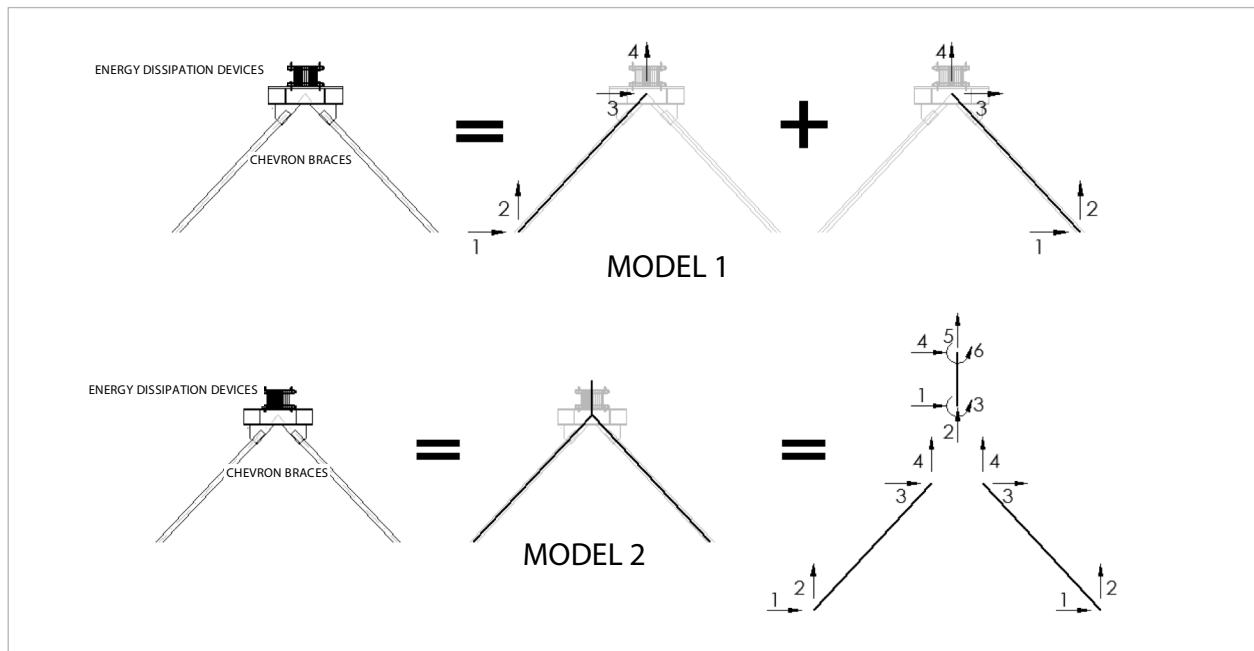


Figure 2. Models developed by the set of dissipating device-brace

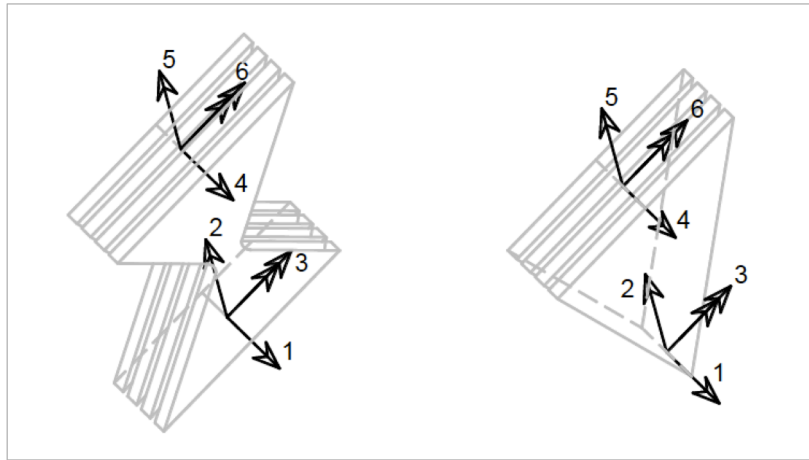


Figure 3. Model 2 A; system of global coordinates of the dissipating element

However, in model B, the keystone methods were used, as shown in Figure 4; the rigidity matrix of each keystone is found, as if it were an element of the constant section; then the rigidity matrix of the direct assembly is obtained and finally the exterior coordinates are condensed as shown in Figure 4.

Table 1 describes the programs used for the two calculation models, indicated in Figure 2; Model 2 programs for A and B are indicated.

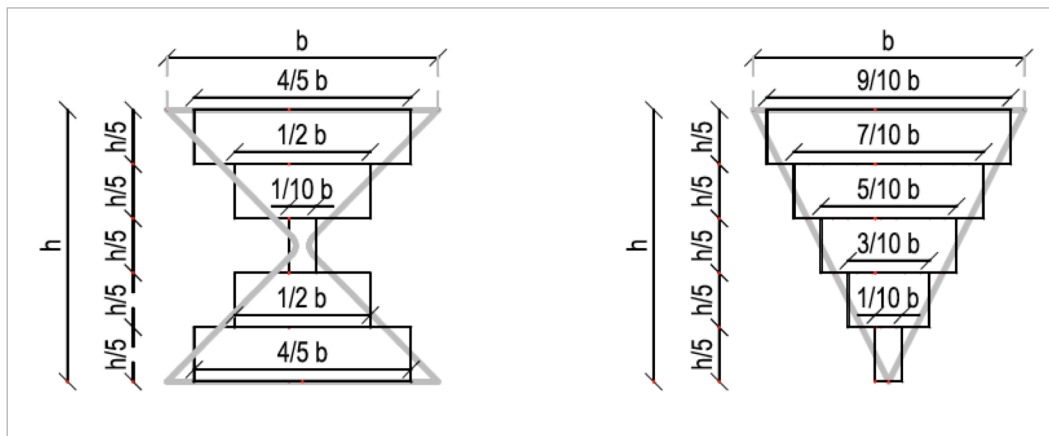


Figure 4. Model 2 B; keystones considered in the ADAS and TADAS dissipating devices

Table 1. Programs that determine the rigidity of the dissipating device over braces, according to the two calculation models

Program	Description
hysteresis_adas	Determines secant rigidity, buffering factor and important points of the double-line model of the ADAS dissipating devices.
hysteresis_tadas	Determines secant rigidity, buffering factor and important points of the double-line model of the TADAS dissipating
k_adas123	Finds the rigidity matrix of the ADAS dissipating element in global coordinates
k_tadas123	Finds the rigidity matrix of the TADAS dissipating element in global coordinates
K1_eqcorte	Finds the rigidity matrix of the dissipating element (ADAS or TADAS) considering the element formed of three rectangular sections, each with a constant section.
K1_eqcorte4	In the prior program, the dissipating element is divided into three segments. Then those exterior segments are divided into two sections based on the plastic length
kdiagonal_tadas	Used to find the rigidity matrix of the steel brace; reports a 6 x 6 matrix in which the third and sixth rows (with the columns) is zero
5	Finds the contribution to the rigidity matrix of the dissipating devices modeled as a equivalent brace
krigidez_tadas	Determines secant rigidity, buffering factor and important points of the double-line model of the ADAS dissipating devices.



### 3. Curvature-moment and rotation-moment diagrams

On the left of Figure 5, the moment-curvature diagram defines the elements' non-linear performance; the curve of the first quadrant corresponds to the case in which the traction

structure is in the lower part, and the curve of the third quadrant is the opposite, since the traction structure is in the upper part. The diagram shows three zones: one elastic up to point Y, with rigidity  $EI_e$ , one plastic rigidity  $EI_p$  and a residual rigidity  $EI_r$ .

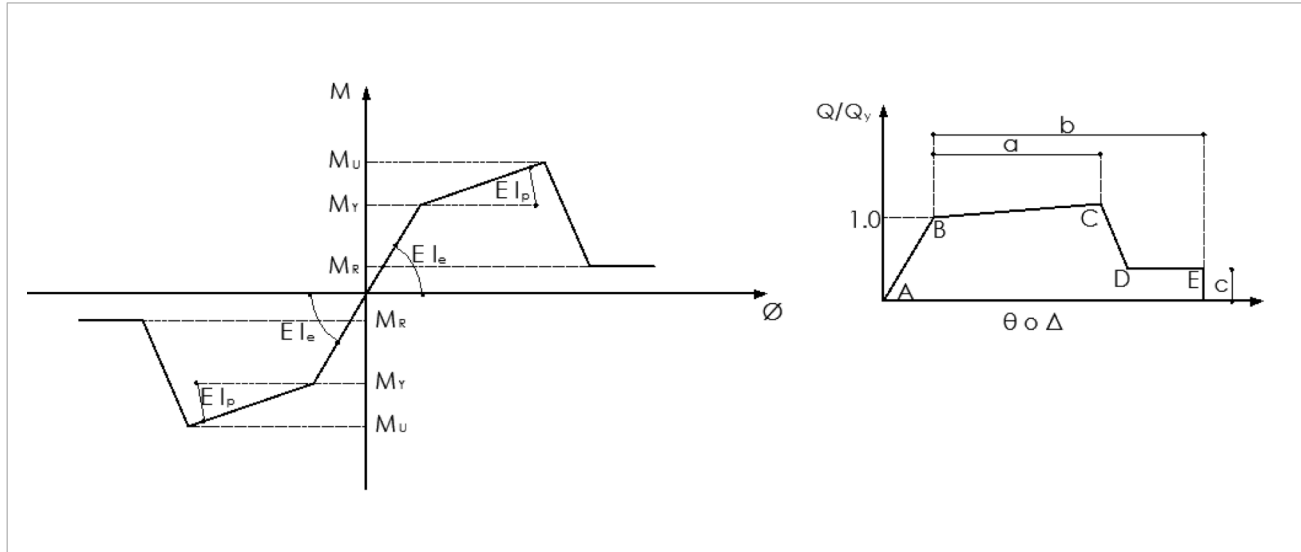


Figure 5. Moment-curvature and moment-rotation diagrams

$$EI_e = \frac{M_y}{\phi_y} \quad EI_p = \frac{M_y - M_r}{\phi_u - \phi_y} \quad EI_r = \frac{M_r}{\phi_y} \quad (2)$$

Where  $M_y, \phi_y$  is the moment and curvature at the point of fluency, based on the work of Y. Park (1985) which includes theoretical and experimental support based on an essay of 400 elements.  $M_u, \phi_u$ , are the moment and curvature in the last point located at the base of the recommendation of ASCE 41 from 2013;  $\alpha$  is the relationship between the post-yield rigidity versus the elastic rigidity.

The right side of Figure 5 shows the important points of the moment-rotation diagram. Point B corresponds to the yield; C at the end, and segment  $\overline{DE}$ , are the R point (residual moment). ASCE 41 provides the variables  $a, b, c$ , which are used to find points C and E; from the yield point, for some steel sections and for reinforced concrete.

Aguiar (2015) details the way to find the residual rigidity through structural analysis, which is valid up to a

rotation less than or equal to  $b \theta_y$ ; the  $b$  coefficient reports ASCE 41 and  $\theta_y$  is the rotation at the yield point.

The step from rotation to curvature is done with longitudinal plastic  $L_p$ , therefore when the section enters the non-linear range, the plastic longitude is obtained based on the moment diagram (Ger and Cheng, 2012).

The calculation was described, only for yield; however for axial force, the steps are similar, but the yield moment is reduced due to axial weight (Li, 2007; the calculation is indicated in Aguiar et al. 2015). Table 2 describes the programs that define the non-linear behavior of the elements, the different elements in the structure, and their contribution to the rigidity matrix of the structure.

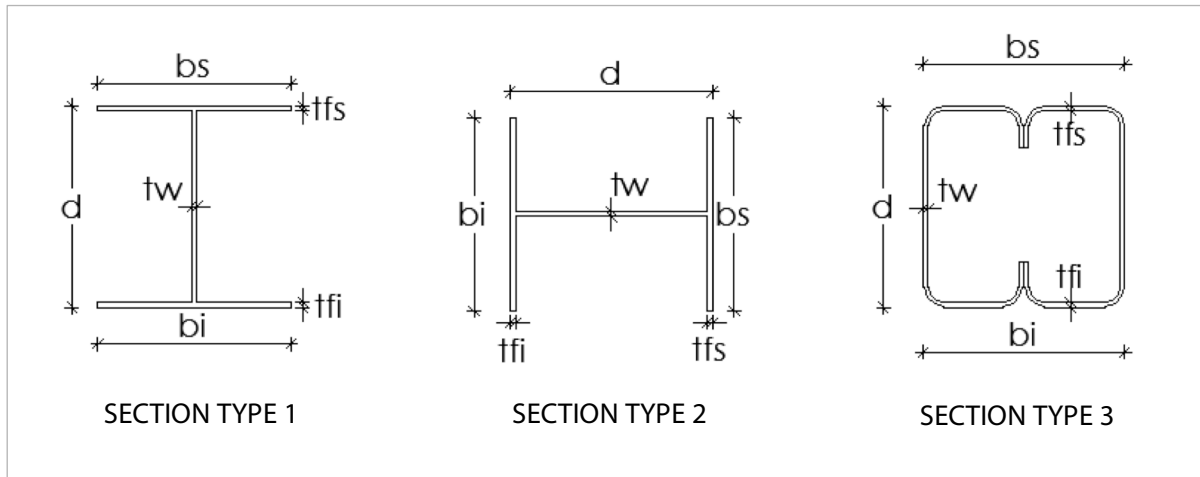


Figure 6. Steel sections programmed in CEINCI-LAB

Table 2. Programs to find the elements' contribution to the rigidity matrix of the structure: columns, beams, dissipating devices, steel braces

Program	Description
Momento_Rotacion_ASCE41B	If the moment is positive in the beams, Assup is on the top and Asinf is on the bottom; if not, the structure is inverted. It also uses programs that determine the ASCE 41 parameters.
Momento_Rotacion_ASCE41C	Similar to the prior program, but now for columns, involving the axial load.
Momento_Rotacion_ConcrASCE41B	Determines the ASCE 41 parameters for the case of the reinforced concrete beams.
Momento_Rotacion_ConcrASCE41C	Determines the ASCE 41 parameters for the case of reinforced concrete columns.
Momento_Rotacion_AceroASCE41B	Determines the ASCE 41 parameters for the case of the steel beams.
Momento_Rotacion_AceroASCE41C	Determines the ASCE 41 parameters for the case of steel columns.
krigidez_ASCE41-2Mfi	Goes from the moment-rotation relationship to the moment-curvature, and it finds yield rigidities in the initial node, center of light, and the final node; this is used to find the rigidity matrix of the beam and column elements using the Giberson model; this composes the structure's total rigidity matrix.
krigidez_braces_eq	Determines the axial rigidity equivalent to the brace-dissipating device. It can be calculated without the dissipating device, and only with braces.
krigidez_damper2	Obtains the rigidity of the dissipating device with model 2 A ,and is added to the structure's rigidity matrix.
krigidez_damper3	Similar to the prior program, but with model 2B
PlasticHinge	Determines the plastic length.
AxialTADAS	Identifies the brand with axial rigidity, for the bilinear strength-displacement model of the TADAS dissipating element.
AxialADAS	Similar to the prior one, but with the ADAS dissipating device

## 4. Monotonic Pushover

The programs that are required for the static structure analysis with CEINCI-LAB are described in Aguiar (2014) so they will not be presented here. In the case of the non-linear analysis, what changes is the rigidity of the sections, according to the branch of the moment-curvature diagram where they are located (ATC 40 ,1996; Chopra ,2014 ) ; the programs for this were described in the prior two sections.

For the Pushover analysis, first the structure under vertical loads is resolved, and the moments and forces, in the elements in local coordinates, are obtained. Then the lateral load cycles start; for this, a very small basal shear  $V_0$  is applied, and this is distributed in each of the floors according to the first vibration and weight mode, FEMA 440,2005.

Where  $V_0$  is the basal shear used for each load cycle.  $w_i$  is the weight of the floor. Note that we are only working with the first vibration mode  $\phi$ , so the sub-index  $i$  corresponds to the floor.

If the basal shear used is very small, the calculation will be more exact but it will take more time to implement. If you want the basal shear  $V_0$ , the user should enter the Pushover\_2 program and set the value of the DeltaV variable, which is the shear  $V_0$ . On the other hand, one of the collapse criteria in the program is that if the global shift is greater than 4% of the total height of the building, it will produce a collapse. The global shift is defined as the ratio between the maximum lateral displacement versus the total height. In the Pushover\_2 program, the global shift variable is *derg*.

$$F_i = \frac{w_i \phi_i}{\sum w_i \phi_i} V_0 \quad (3)$$

**Table 3.** Description of the programs to use Pushover

Program	Description
Geom	It determines the properties of the elements such as the area, inertia moment, yield moment, axial rigidity yield and rigidity yield
Structure_Geom_2D_v2	The program determines the geometry of a structure, the degrees of freedom, the matrix that has the placement vectors, the length, sine and cosine of the elements.
Pushover_2	The program that obtains the seismic resistance capacity curve of frames, with and without ADAS and TADAS dissipating devices.
Iteration_Vy	Its function is to exactly determine the yield point in a section (when the moment in the moment-curvature diagram gets over the elastic zone). It goes back one cycle and reduces the load increase.
Dibujo_Din	Draws each lateral load cycle and the structure, and places the plastic hinges. Using this program requires more time.
Dibujo_Din2	This program provides the option to indicate how many load cycles; draws the structure and uses colors to color the elements to indicate the zone where it is located. Green is for the post-shear zone, and red is the residual zone.
masas2	Find the mass matrix in the model that considers the dissipating device to be another element. On the lower part, there is no mass so its value is zero.
masas	Determine the mass matrix for the model using the equivalent brace to the brace-dissipating device set.
fuerzas_0	Find the forces in local coordinates, in each load cycle. Then they are stored in Table 2

ENGLISH VERSION.....

Table 3 presents the programs used to obtain the seismic resistance capacity curve.

The opening files required to use the programs are in the matrices described in Section 7 of this paper; then, you write the name of the main program such as Structure\_Geom\_2D\_v2 y Pushover\_2.

The program Structure\_Geom\_2D\_v2 calls the various programs used to build the structure, which are detailed in Aguiar (2014). Other missing programs that haven't been mentioned yet are Initialization, which sets some variables and equations at zero. Aguiar (2013) includes another complement to the programs used in the CEINCI-LAB computing system.

## 5. Concrete structures analyzed

On the left side of Figure 7, a 4- floor structure is

presented, with columns of 50/50 cm. and beams of 40/40; this is the same for all floors. The vertical load on each floor is 0.75 T/m. On the right side of the Figure, typical structures of a column and beam are shown. The cross-sections of the Chevron braces are 100/100/10 mm. The elastic modulus of the concrete is 1500000 T/m<sup>2</sup>.

Steel dissipating devices have been installed on the first three floors, as indicated in Figure 8. The one on the first floor has 6 layers; the ones on the second and third floor have 4 layers, both for ADAS and TADAS. The thickness of the plates is 1 cm.; this size was used to fit within the non-linear range.

The seismic resistance curve will be calculated, first with the ADAS, and then with the TADAS dissipating devices.

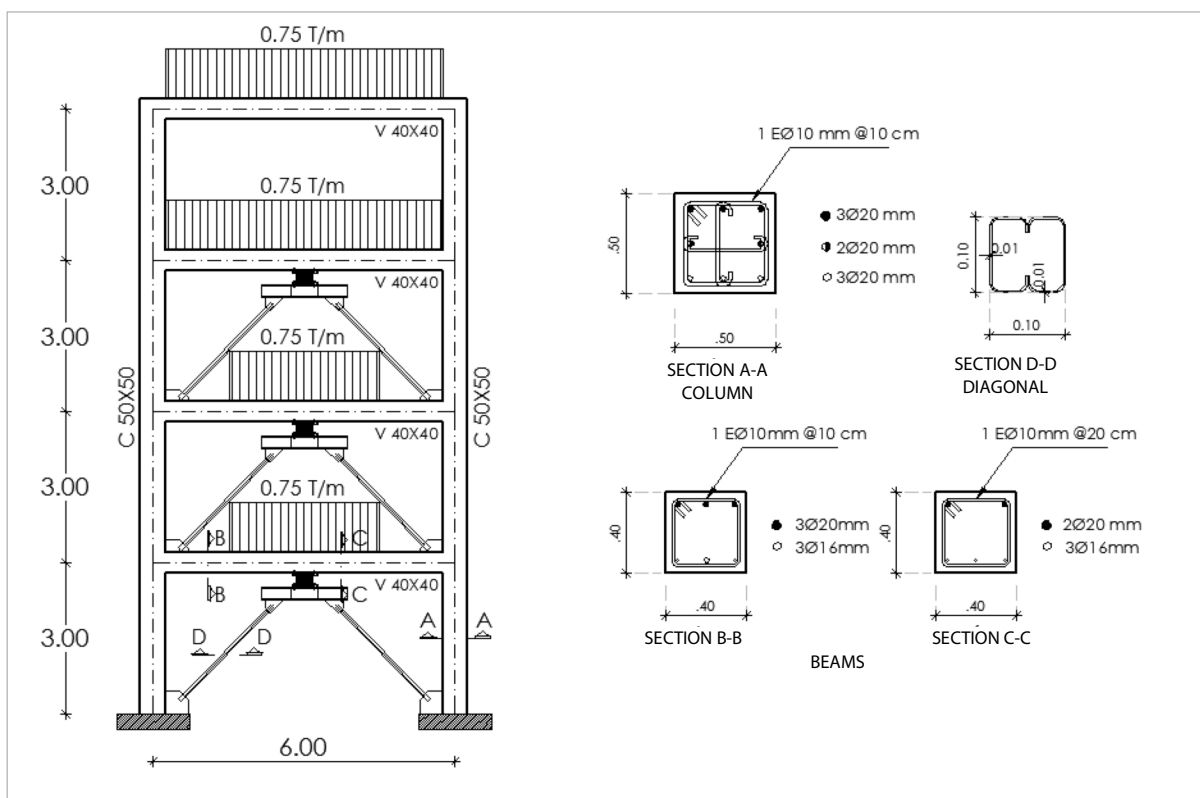


Figure 7. Analysis of reinforced concrete structure

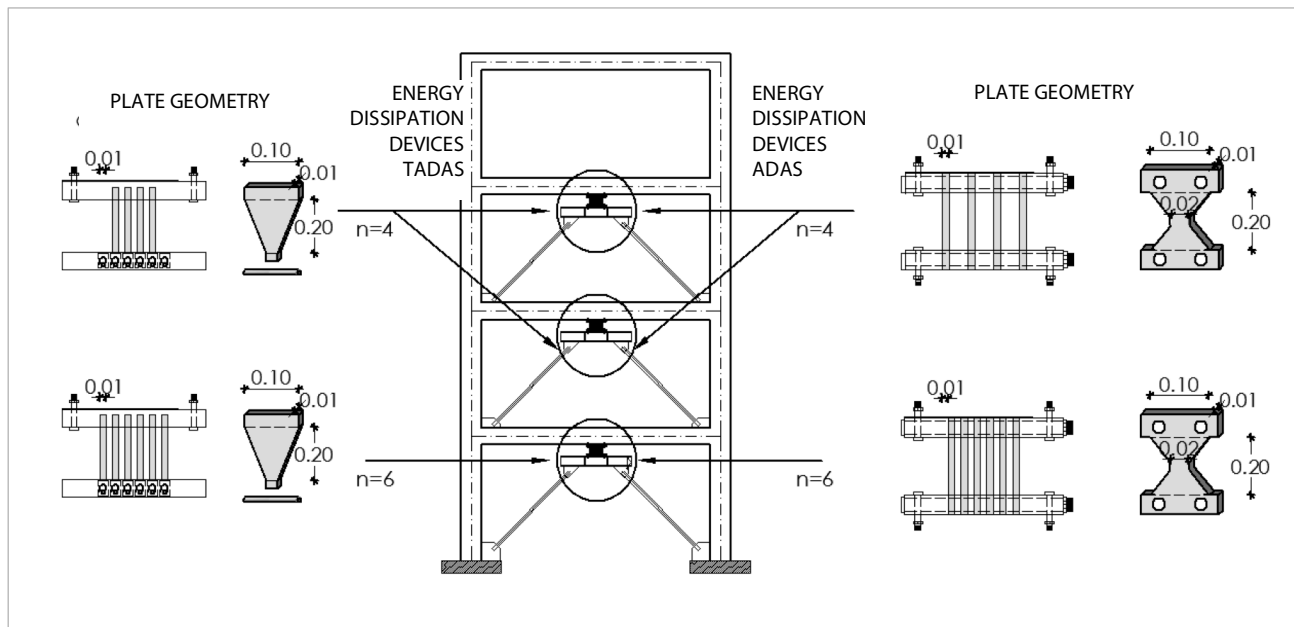


Figure 8. Geometry of the dissipating devices considered for the first three floors. The left side shows ADAS and the right side shows TADAS

For Model 1 with equivalent braces, there are 26 degrees of freedom, as indicated in Figure 9. The left side of the Figure shows the numbering of the nodes and elements. Note that first numbering is assigned to all of the concrete elements and then to the equivalent braces; this way it is easier to sum the rigidity matrix of the concrete elements and the steel elements. The 4/4 mass program is used to find the mass matrix of this model.

Figure 10 shows Model 2, where the dissipating device is another element in the structure. In this case, the main coordinates (lateral) are 7; the mass and rigidity matrices are 7/7. The mass matrix elements (1,1): (3,3) and (5,5) are zero, since there is not weight at those points. The load gravitates to the floor, and therefore the program used is masas2.

The seismic resistance capacity curves with the ADAS

dissipating devices are presented in Figure 11, and the TADA dissipaters in Figure 12. In both cases, the curves are shown that were calculated with with SAP 2000 and ETABS V15. Appendix A details how the dissipating devices were modeled for each of the cases. Note that the results found with SAP 2000 and ETABS V15, shown in these figures, are similar to those found with Model 1.

The objective of this article is to show the use of the CEINCI-LAB computer system in finding the seismic capacity curve in frames with ADAS or TADAS energy dissipating devices.

The names of the programs that calculate the seismic capacity curve with the equivalent braces model are: MON4p\_ADASeq y MON4p\_TADASeq. When the dissipating element is used, the programs are: MON4p\_ADAS y MON4p\_TADAS.

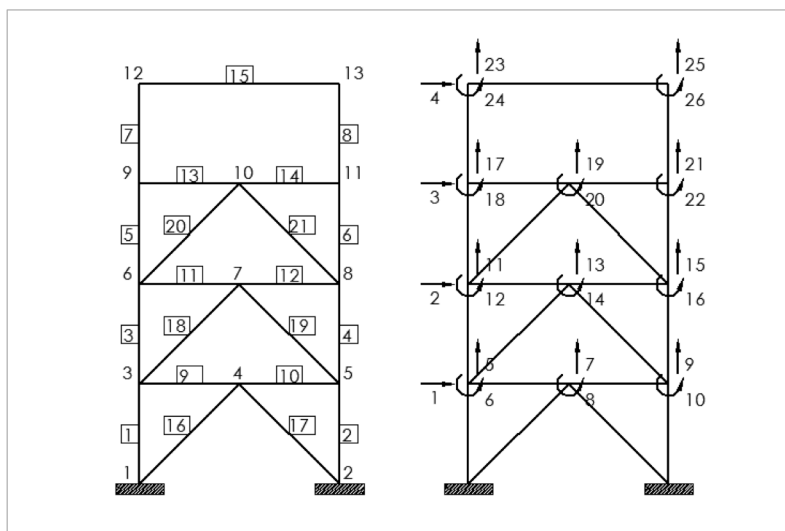


Figure 9. Geometry of the dissipating devices considered for the three first floors; ADAS shown on the left and TADAS shown on the right



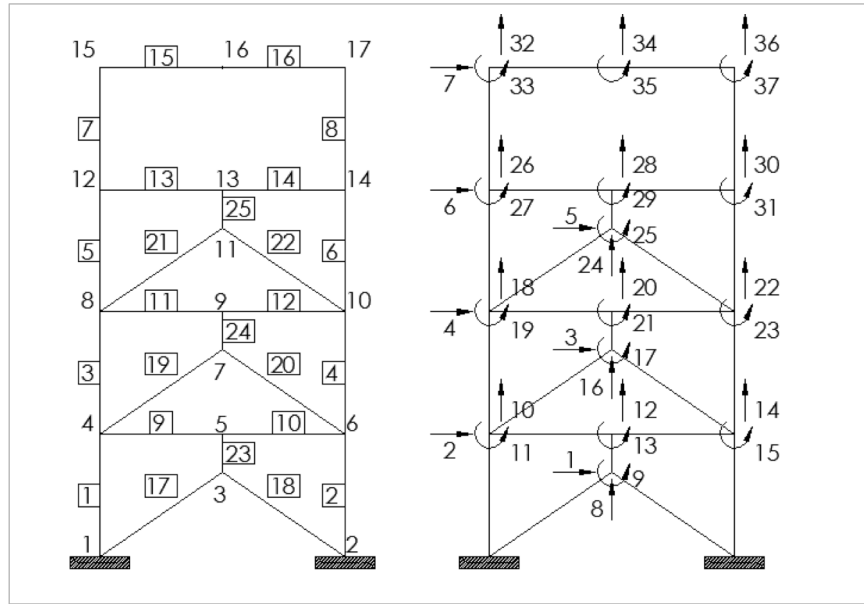


Figure 10. Numbering of nodes, elements and degrees of freedom - Model 2

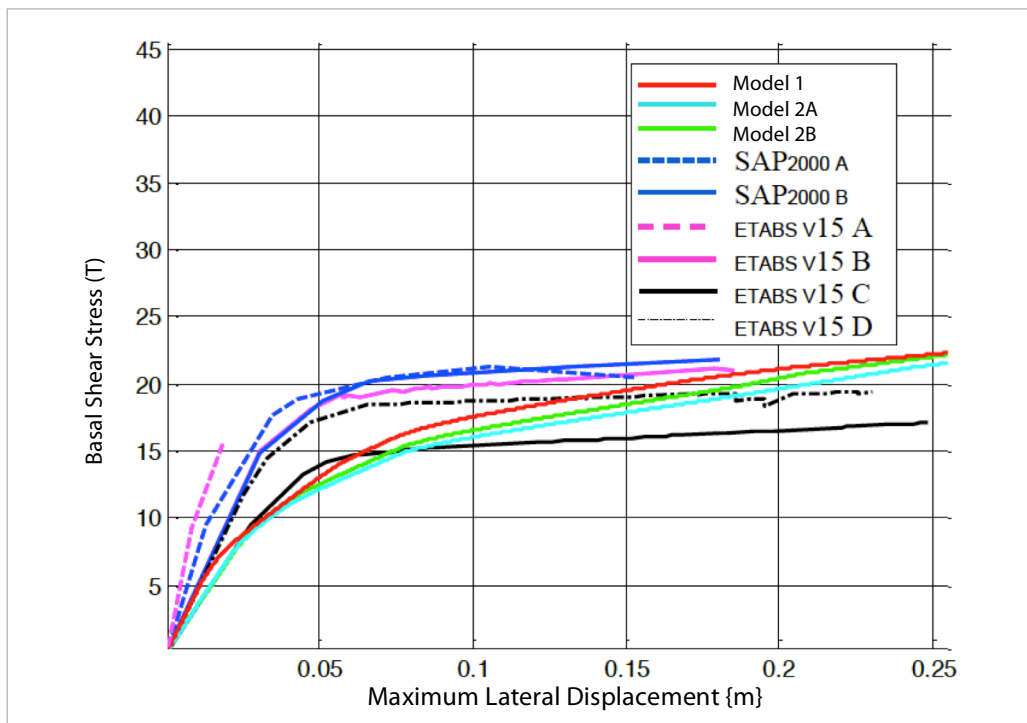


Figure 11. Seismic resistance capacity curves with ADAS dissipating devices

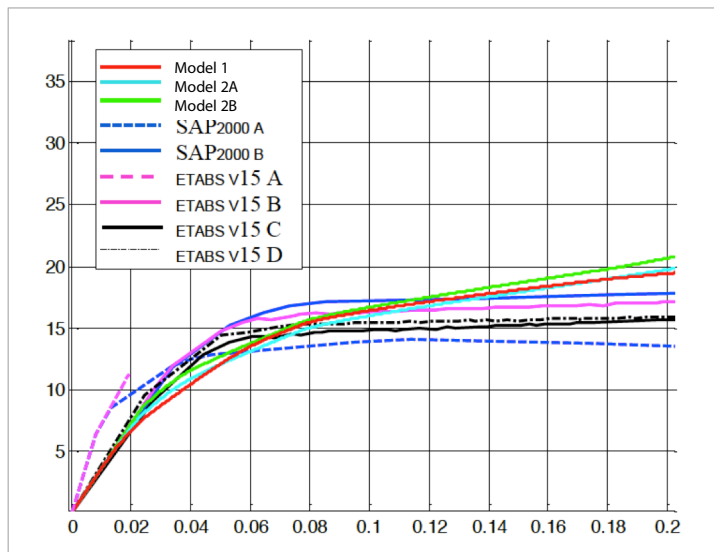


Figure 12. Seismic resistance capacity curves with TADAS dissipating devices

## 6. Steel structure

A heat-laminated steel structure of 6 floors is analyzed, with energy dissipating devices placed in the main span of each of the floors, as shown in Figure 13. They use profiles type “I” and “H.” The first one corresponds to the flange width in inches and the second one is the weight by unit of length (lbr/ft). The sections of the profiles are symmetrical, which is different than the reinforced concrete structure analyzed in the prior section.

The energy dissipaters for the first three floors are the same, and they have 10 plates; the rest are different. Figure

14 indicates their geometry, both for ADAS and TADAS. The numbering of the nodes and elements used in the programs are MON6p\_ADAS, MON6p\_TADAS, MON6p\_ADASeq, MON6p\_TADASeq. The first two use a dissipating element and the last two use an equivalent brace. Figure 15 is for Model 1, with an equivalent brace. Figure 16 is for Model 2, which includes the energy dissipating device as another element within the structure. These figures also present the structures’ degree of freedom.

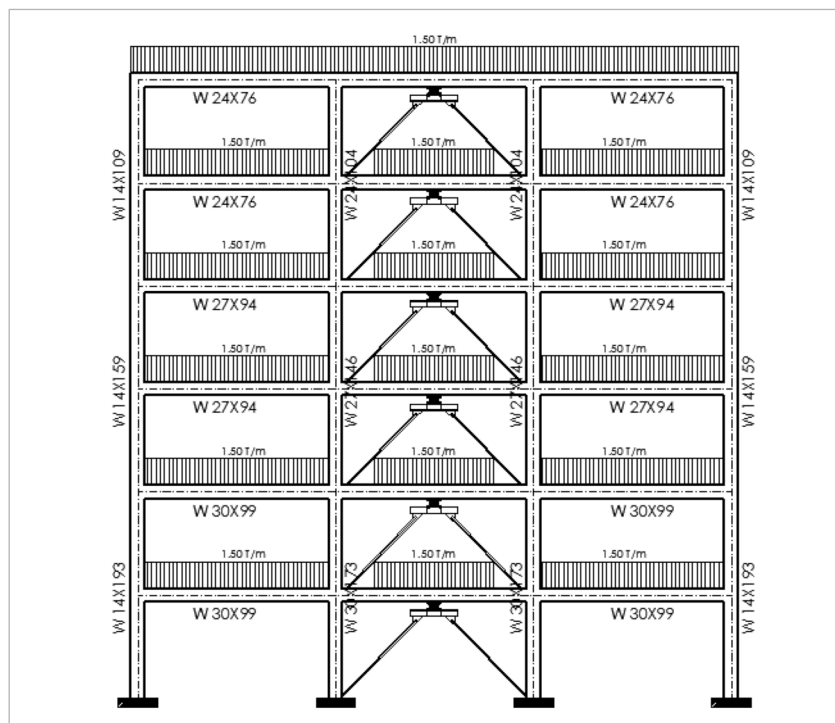


Figure 13. Steel structure with energy dissipating devices



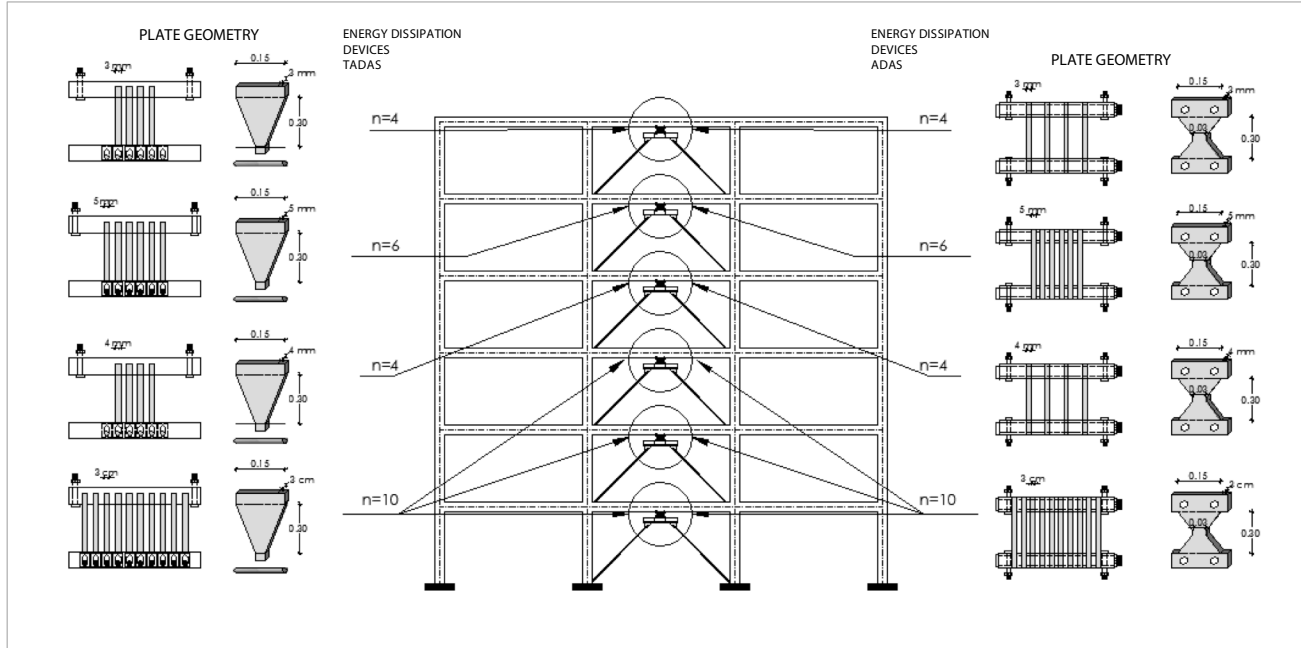


Figure 14. Geometry of the dissipating devices used for the steel structure

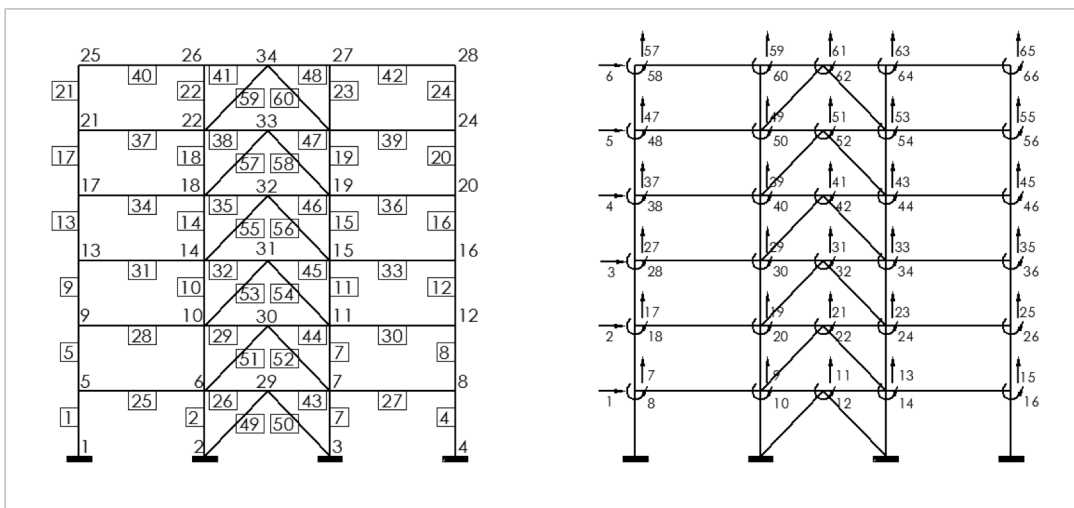


Figure 15. Number of nodes, elements and degrees of freedom for Model 1

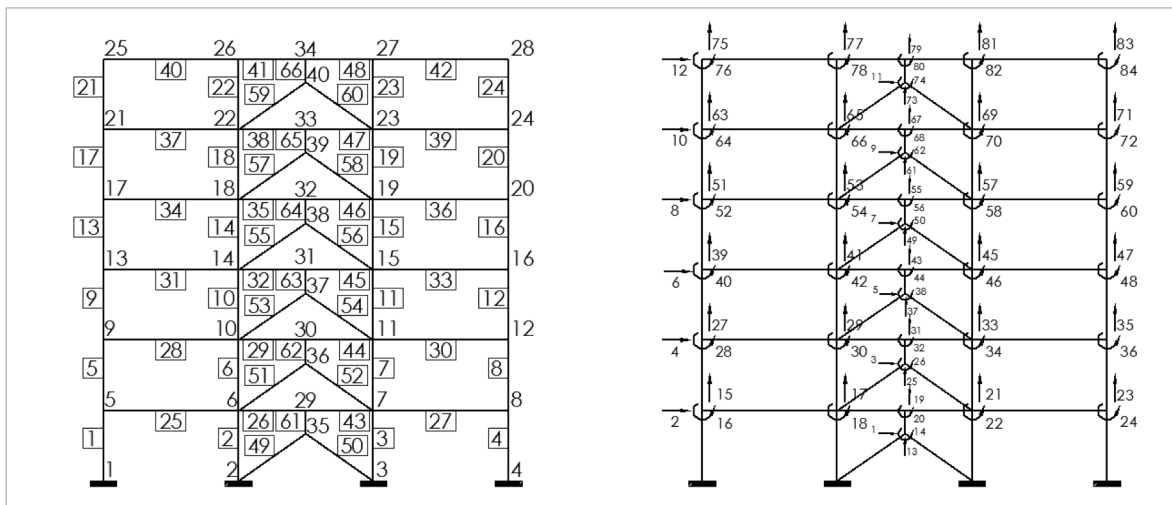


Figure 16. Numbering of nodes, elements, and degrees of freedom for Model 2



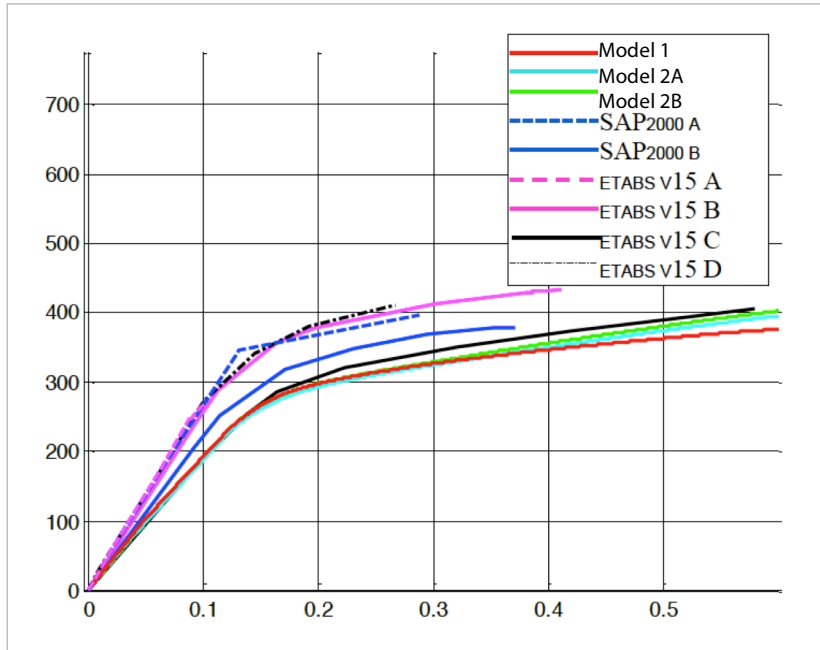


Figure 17. Seismic resistance capacity curve found in a steel structure with ADAS dissipating devices

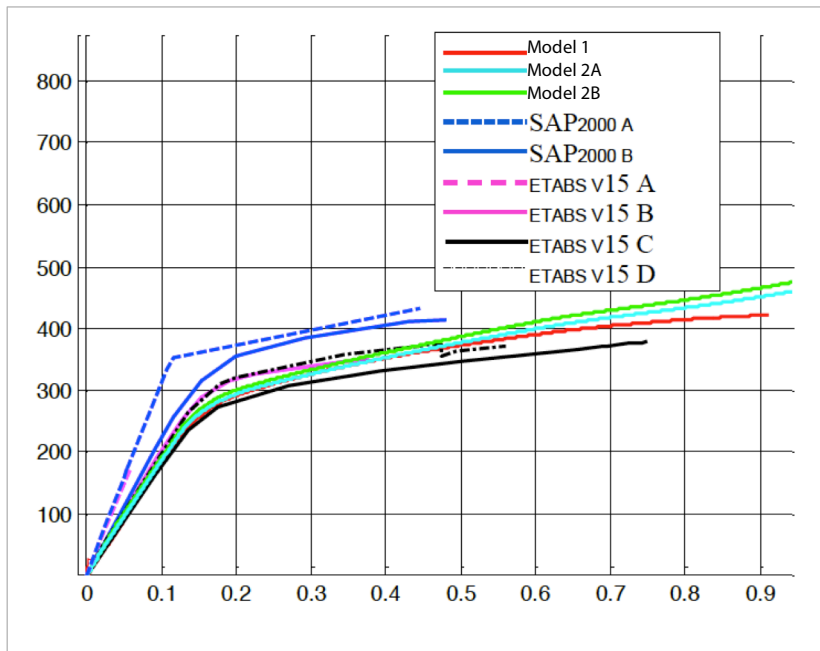


Figure 18. Seismic resistance capacity curve found in a steel structure with TADAS dissipating devices

ENGLISH VERSION.....

With the models 2A and 2B, practically the same curves are obtained; the difference is minimal, giving the impression of being just one curve. Model 1 shows lower values but they are similar to the values found with other models.

The ETABS V15C model provides results that are very similar to those found with other models, specifically models 1, 2A and 2B, especially for the case of ADAS. The ETABS 15D model also reports similar results. In Appendix A, there is a detailed description of the models used in the ETABS and SAP 2000 programs; in general, we can state that they generate similar values, comparable with those found with the CEINCI-LAB computer system.

The programs presented in this article show tables that indicate the sequence of the elements that get into the nonlinear range (with the moment in the moment-curvature diagram gets over the elastic zone) is shown, and has subroutines that display the sections where plastic hinges have been formed.

On the other hand, with these programs, we can do a seismic analysis of reinforced concrete structures or steel with braces in the shape of an inverted "V" without energy dissipaters or simply with braces.

Likewise we can obtain the seismic capacity resistance curve in structures that had ADAS or TADAS energy dissipaters installed on the beams, without a need for Chevron bracing, such as the Barlovento building that is being built in Lima, Peru.

## 7. Data entry process

The first step is to define the structural element sections: beams, columns and energy dissipating devices, if they are used. Each section definition should indicate the numerical code for the material and the cross-section type; these codes are shown in the table below:

Table 4. Definition of the structural elements

I	TYPE OF MATERIAL	CROSS-SECTION							
		Type 1 Profile	Type H Profile	Tubular Rectangular Profile	Rectangular solid	Rectangular L type	Rectangular T type	ADAS	TADAS
CONCRETE	2	-	-	-	1	1	1		
STEEL	1	1	2	3	-	-	-		
BRACE DISSIPATING DEVICE	1.1	1	2	3					
DISSIPATING DEVICE	1.2							4	5

### 7.1 Steel beams and/or columns

To define a steel section, fields will be used that are

mentioned below, with the name from matrix Table1; each row represents the corresponding number of the element:

Table 5. Matrix Table1 to create steel elements

Name of section	=	Type of material	fy	fu	Ey	Tipo de sección	d	tw	bs	bi	tfs	tfi
To be defined by user	=	As per table 4	Elastic yield of steel	Yield limit of steel	Young's modulus	As per table 1	Alto de la sección	Thickn ess of web	Width of upper flanges	Width of lower flanges	Thickne ss of upper flanges	Thickn ess of lower flanges

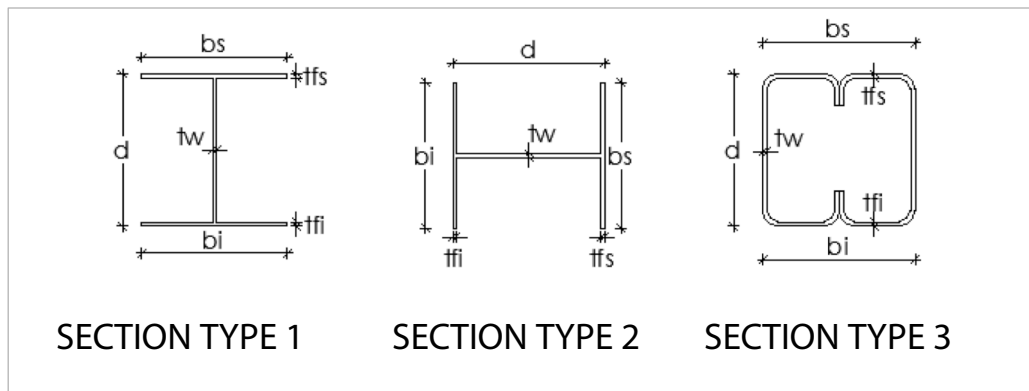


Figure 19. Section types for steel elements

7.2 Concrete beams and/or columns

To define a section of concrete, fields will be used that

are indicated below in Table 1 Matrix; each row represents the number of the corresponding element:

Table 6. Table1 Matrix for reinforced concrete elements

Name of section	=	Type of material	$f'c$	$E_y$	$f_y$	Sección type	$h$	$b$	$bw$	$tf$
To be defined by user	=	As per table 4	Compressive strength of Concrete	Young's modulus of the reinforced steel	Reinforced steel strength	As per table 1	Height of section	Width of section	Web thickness	Wing thickness

$d'$	$As_{sup}$	$As_{inf}$	Stirrup separation	$Av$	$As1$
Distance from extreme compression fiber to centroid of compression reinforcement	Area of upper reinforcement	Area of lower reinforcement	Separation of stirrups	Area of stirrup branches	Area of steel in the middle of the section, in the case of columns

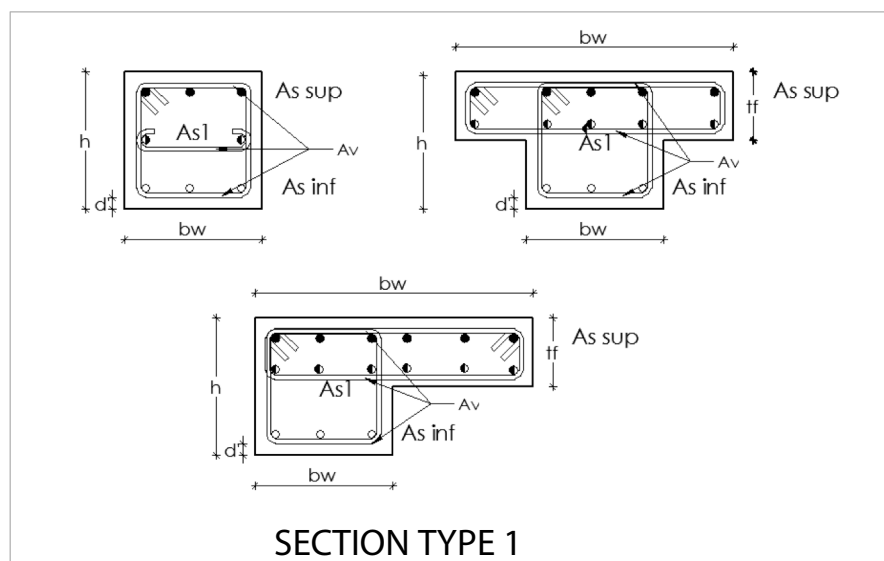


Figure 20. Typical sections for elements of reinforced concrete

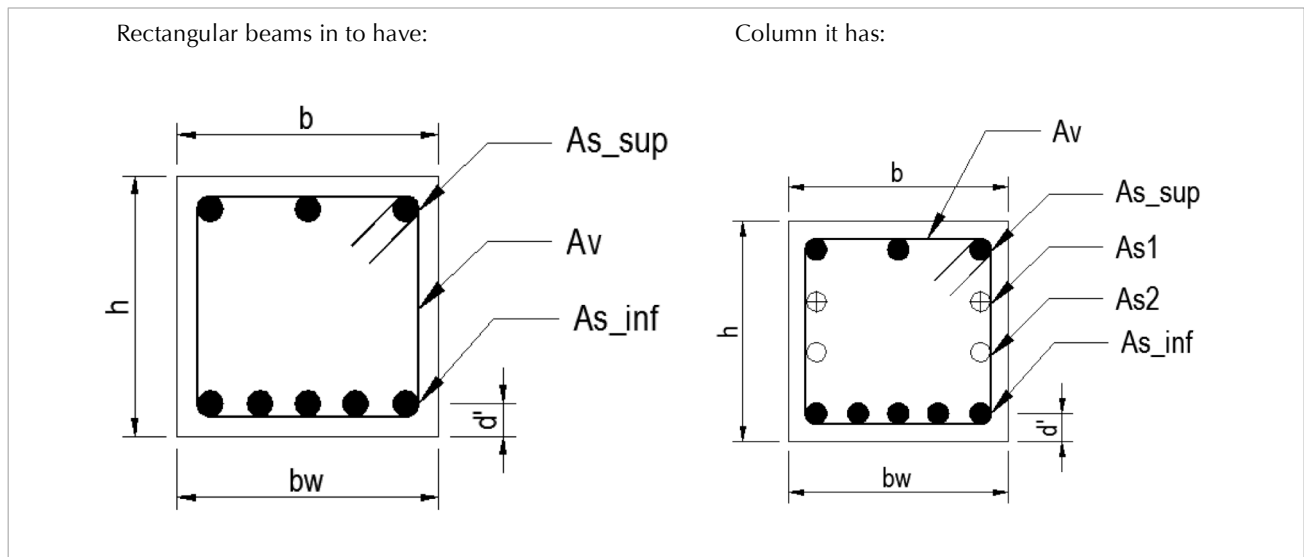


Figure 21. Information about the reinforcement of beams and columns

### 7.3 ADAS and TADAS dissipating devices

Table 7. Table1 Matrix to create ADAS dissipating devices

Section name	=	Type of material	fy	fu	Es	Type	h	tw	bs	bi	n	miu
To be defined by user	=	As per Table 4	Yield limit	Platic limit	Steel elastic modulus	Type 4 ADAS	Height of the plate	Thickness of the plate	Upper base	Upper base	Number of plates	Flexibility of the dissipating device

Table 8. Table1 Matrix to create TADAS dissipating devices

Section name	=	Type of material	fy	fu	Es	Type	h	tw	bs	b	n	miu
To be defined by user	=	As per Table 4	Yield limit	Platic limit	Modulus of elasticity of steel	Type 5 TADAS	Height of the plate	Thickness of the plate	Upper base	Base of the middle section	Number of plates	Flexibility of the dissipating device

## 8. Comments and conclusions

The CEINCI-LAB computer system provides an easy-to-use way to find the resistant seismic capacity curve resistance of the flat frames of reinforced concrete or steel, with ADAS or TADAS energy dissipaters placed on top of Chevron bracing. The most important aspects of the theoretical framework were briefly presented, and the programs used to resolve these topics were covered, allowing the reader to have an understanding of these topics.

In the examples reviewed, the seismic capacity curve compares the basal shear with the maximum lateral displacement; the curves obtained by the equivalent brace model for the set of brace-dissipation devices report shear

forces that are smaller than the model that considers the energy dissipation device as an additional element. Two models were presented: one corresponds to an analytical solution of the rigidity matrix of the ADAS dissipating device and the quasi-analytical solution for the TADAS dissipater, and the other is an approximate solution that considers segments of constant sections in the dissipating devices. For these two models, the examples show a close approximation of seismic capacity curves.

The programs related to the topics reviewed in this article are located in the dropbox, in the following website: [www.espe.edu.ec](http://www.espe.edu.ec). In this manner, we are contributing to the development of Seismic Engineering.



## 9. Appendix A

For the SAP2000 A and ETABS V15 C models: the energy dissipating device was modeled as an element type frame with that shape, an equivalent thickness to the yield moment, and the behavior of the plastic hinges as flexo-compression from automatic tables of ASCE-41 code.

For the SAP2000 B and ETABS V15 B: the equivalent brace was remodeled as a link type multilinear element controlling their behavior by modeling strength - Axial strain curve of the form shown in Figure A1.

$$q_{ty} = q_{y \text{ diagonal}} + q_{y \text{ disipador}}$$

$$q_{tu} = q_{y \text{ diagonal}} + q_{u \text{ disipador}}$$

$$F_{ty} = Keq_e * q_{ty}$$

$$F_{tu} = F_{ty} + Keq_p * (q_{u \text{ disipador}} - q_{y \text{ disipador}})$$

For the ETABS V15 C model: a multilinear link type element is modeled, controlling its performance with a Strength-Strain axial curve and the Shear-Strain curve as follows:

$$k_{Ae} = E * A_{\text{disipador}} / h_{\text{disipador}} * A_{\text{disipador}}$$

= smaller área of the dissipating device

$$h_{\text{disipador}} = \text{height of dissipating device}$$

$$k_{Ap} = 0.03 k_{Ae}$$

$$q_{dy} = \frac{f_y}{E * h}$$

$$q_{du} = \mu * q_{dy}$$

$$F_{dy} = K_{Ae} * q_{dy}$$

$$F_{du} = F_{dy} + Keq_p * (q_{du} - q_{dy})$$

$$V_{dy, du} = \text{Shear strength limit}$$

$$d_{dy, du} = \text{displacement limits in the shear forces' direction}$$

$$M_{dy} = V_{dy} * h_{\text{disipador}} / 2$$

$$M_{du} = V_{du} * h_{\text{disipador}} / 2$$

$$\theta_{dy} = d_{dy} / h_{\text{disipador}}$$

$$\theta_{du} = d_{du} / h_{\text{disipador}}$$

For the ETABS V15 D model: the equivalent brace was modeled as an element type pinned frames with an area of  $Aeq_e = k_{Ae} / E$ , controlling its performance with the allocation of plastic hinges; includes axial Strength-Strain curve models as indicated in models SAP2000 B and ETABS V15 B.

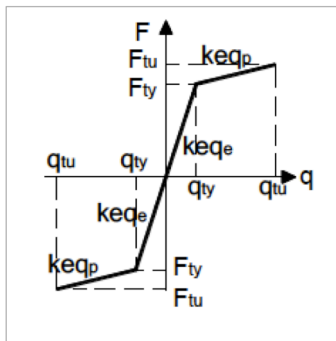


Figure A1. Information about the beam and concrete reinforcement

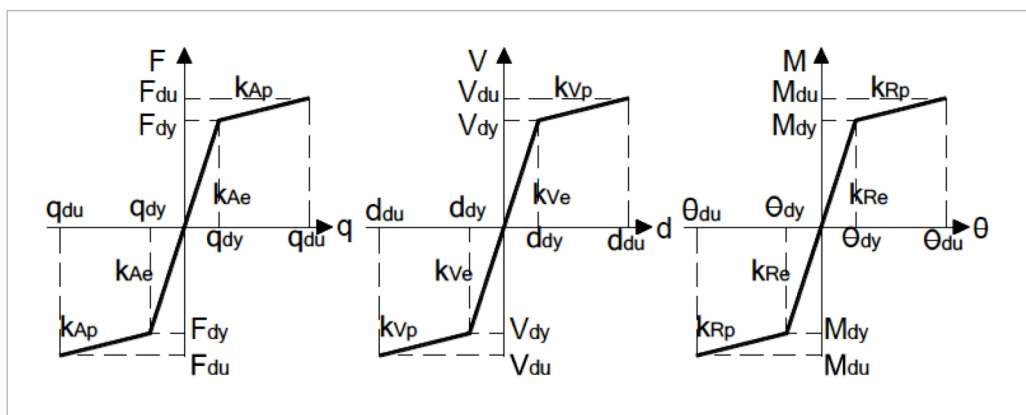


Figure A2. Strength-Axial Strain Curve, Shear-Strain in the shear direction curve, and Moment-Rotation curve



## 10. References

- AISC-360 (2010)**, Specification for Structural Steel Buildings. American Institute of Steel Construction (AISC).
- Aguilar R., Rodríguez M., Mora D. (2015,1)**, Análisis sísmico de estructuras con disipadores ADAS o TADAS, Presentado para su publicación en la Serie Monografías en Ingeniería Sísmica. Centro Internacional de Métodos Numéricos en Ingeniería CIMNE, Universidad Politécnica de Cataluña, Barcelona, España.
- Aguilar R., Mora D., Morales E., (2015,2)**, "Peligrosidad sísmica de Quito y el método del espectro de capacidad con CEINCI-LAB", Revista Internacional de Ingeniería de Estructuras, 20 (1), 1-39.
- Aguilar R. (2014)**, Análisis Matricial de Estructuras con CEINCI-LAB, Universidad de las Fuerzas Armadas, Instituto Panamericano de Geografía e Historia IPGH. Cuarta edición, 676 p.
- Aguilar R. (2012)**, Dinámica de estructuras con CEINCI-LAB, Universidad de las Fuerzas Armadas, ESPE. Segunda Edición, 416 p.
- ASCE 41 (2013)**, Seismic rehabilitation of existing buildings, American Society of Civil Engineers ASCE/SEI 41-13.
- ATC-40 (1996)**, "Seismic evaluation and retrofit of concrete buildings", Applied Technology Council, Redwood City, California.
- Chistopoulous C. y Filiatraul A. (2006)**, Principles of passive Supplemental Damping and Seismic Isolation. IUSS Press, Instituto Universitario di Studi Superiori di Pavia, Pavia, Pavia, IT.
- Chopra A. K. (2014)**, Dynamic of Structures Theory and application to earthquake engineering. 4th edition.
- FEMA 440 (2005)**, Improvement of Nonlinear Static Seismic Analysis Procedures, Federal Emergency Management Agency, FEMA 440.
- Ger y Cheng (2012)**, Seismic Design Aids for Nonlinear Pushover Analysis of Reinforced Concrete and Steel Bridges.
- Heresi Pablo (2012)**, Comportamiento de placas de CuZnAl para disipadores tipo ADAS. Tesis de Maestría. Universidad de Chile, 141 p.
- Hernández Eliud (2009)**, Análisis No Lineal – Pushover, CSI.
- Holzer et al. (1975)**, SINDER. A Computer Code for General Analysis of Two-Dimensional Reinforced Concrete Structures. Report. AFWL-TR-74-228 Vol. 1. Air Force Weapons Laboratory, Kirtland, AFB, New Mexico.
- J.S. Chiou1, H.H. Yang2 y C.H. Chen (2008)**, Plastic hinge setting for nonlinear pushover analysis of Pile foundations, The 14th World Conference on Earthquake Engineering.
- Kotulka, Brandon A. (2007)**, Analysis for a Design Guide on Gusset Plates used in Special Concentrically Braced Frames, Master of Science in Engineering Thesis, University of Washington
- Li Guo-Qiang (2007)**, Advanced Analysis and Design of Steel Frames.
- Mora D. y Aguilar R. (2015)**, "Modelación del diagrama momento-curvatura y momento rotación en secciones de acero estructural", Revista Ciencia, 17 (1), 101-128.
- Park Y. (1985)**, Seismic damage analysis and damage-limiting design for reinforced concrete structures, Ph.D. Thesis, Department of Civil Engineering, University of Illinois at Urbana-Champaign.
- Powell Graham H. (2013)**, Curvature as a demand – capacity measure.
- Tena A. (1997)**, "Mathematical modelling of the ADAS energy dissipation device", Engineering Structures, Vol. 19, No. 10, pp. 811-821.
- Tena A. (2000)**, "Modelado analítico de edificios con disipadores de energía", Revista de Ingeniería Sísmica, SMIS, No. 62, pp. 29-62, enero-junio.
- Tena A. (2009)**, Análisis de estructuras con métodos matriciales, Editorial Limusa, Primera edición, 559 p., México.
- Tsai K-C., Chen H-W., Hong C-P. y Su Y-F. (1993)**, "Design of steel triangular plate energy absorbers for seismic-resistant construction", Earthquake Spectra, 9 (3), 505-528.
- Web.MIT.edu**, Moment – Curvature, Beam Review.
- Wittaker A.S., Bertero V., Alonso L., y Thompson C. (1989)**, Earthquake simulator testing of steel plate added damping and stiffness elements, Report UCB/EERC-89/02. Earthquake Engineering Research Center, University of California at Berkeley.

